INTEGRAL

Science Operations Centre

Announcement of Opportunity for Observing Proposals (AO-6)

OMC Observer's Manual

INT/OAG/08-0296/Dc

Issue 1.0

10 March 2008

Prepared by E. Kuulkers

Authorised by A.N. Parmar

Based on inputs from M. Mas Hesse (OMC PI, INTA/LAEFF), A. Domingo Garau (OMC team, INTA/LAEFF) and P. Kretschmar (ISOC, ESA/ESAC)

Table of Contents

1 Introduction

The Optical Monitoring Camera (OMC) is a wide-field optical instrument using a large-format CCD detector, limited by a relatively low telemetry rate. It measures the optical emission from the prime targets of the two gamma-ray instruments SPI and IBIS. The OMC offers the first opportunity to make observations of long duration in the optical band simultaneously with those at hard X-rays and gamma-rays. Multi-band observations are particularly important in high-energy astrophysics where variability is typically rapid, unpredictable and of large amplitude. The main objectives of the Optical Monitoring Camera can be summarised as follows:

To monitor during extended periods of time the optical emission of all high-energy targets within its field of view, simultaneously with the high-energy instruments.

To provide simultaneous and calibrated standard V-band photometry of the high-energy sources to allow comparison of their high-energy behavior with previous or future ground-based optical measurements.

To analyse and locate the optical counterparts of high-energy transients detected by the other instruments, especially gamma-ray transients.

To monitor any other optically variable sources serendipitously within the OMC field of view, which may require long periods of continuous observations for their physical understanding (variable stars, flaring and eruptive objects, etc.).

The purpose of this manual is to present all the information about the OMC which is necessary for the preparation of Integral proposals. A more detailed description of the instrument can be found in the OMC Analysis Scientific Validation Report, part of the OSA documentation (http://isdc.unige.ch/index.cgi?Soft+download).

Table 1: OMC parameters and scientific performances

Parameter	**In-orbit value**
Field of view	4.979° × 4.979°
Aperture	5 cm diameter
Focal length	153.7 mm (f/3.1)
Optical throughput	> 70% at 550 nm
Stray light reduc. factor[1] (within UFOV[2])	<< 10^{-4} (no stray light detected)
Angular resolution	≈ 23" Gauss PSF (FWHM=1.3±0.1 pix)
Point source location accuracy	≈ 2"
Angular pixel size	17.504"× 17.504"
CCD pixels	2061 × 1056 (1024 × 1024 image area) (13 × 13 μm^2 per pixel)
CCD Quantum efficiency	88% at 550 nm
CCD full well capacity	~ 120 000 electrons/pixel
ADC levels	12 bit signal, 4096 levels: ~30 cts/digital level (low gain) ~5 cts/digital level (high gain)
Frame transfer time	≈ 2 ms
Time resolution	> 3 s
Typical integration times	10 s - 50s - 200 s
Wavelength range	Johnson V filter (centered at 550 nm)
Limit magnitude (10 × 200 s, 3σ) (50 × 200 s, 3σ) (100 × 200 s, 3σ)	18.1 (m_V) 18.9 (m_V) 19.3 (m_V)
Sensitivity to variations (10 × 100 s, 3σ)	$\Delta m_V < 0.1$, for $m_V < 16$

[1]This parameter defines the factor by which the flux from any source within the UFOV (but outside the FOV) is reduced by multiple reflections before reaching the detector surface as background light
[2]The unobstructed field of view (UFOV) defines the angle which has to be clear to space in order to avoid reflected light directly reaching the optics

2 Description of the instrument

2.1 Overall design

The OMC consists of an optical system focused onto a CCD detector. The optics are refractive with an entrance aperture of 5 cm diameter and a square field of view of ≈5° × 5°. A Johnson V filter allows photometric calibration in a standard system. An optical baffle ensures the necessary reduction of scattered sunlight and also the unwanted stray-light coming from non-solar sources outside the FOV. A deployable cover protected the optics from contamination during ground operations and early operations in orbit. It was released during the early steps of the commissioning phase. It now forms part of the baffle. See Figure 1 for a diagram of the OMC.

The camera unit is based on a large-format CCD (2061×1056 pixels) working in frame transfer mode (1024×1024 image area and 1024×1024 storage area, not exposed to light). This design, with a frame transfer time of around 2 ms, allows continuous measurements and makes it unnecessary to have a mechanical shutter. A LED light source within the optical cavity provides "flat-field" illumination of the CCD for on-board calibration.

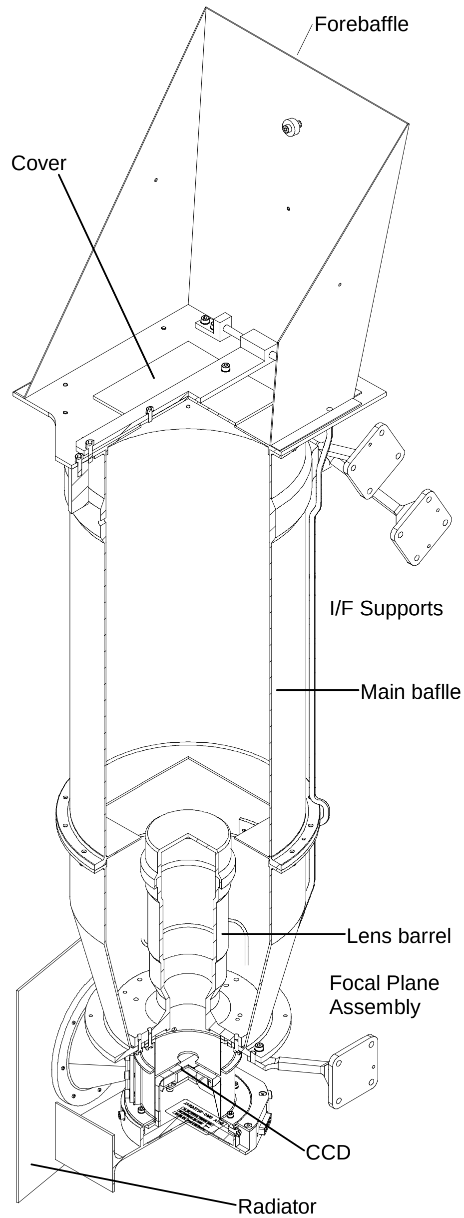

Figure 1: A 3-D cut of the OMC Camera Unit.

2.2 The optics

The optical system, as shown in Figure 2, consists of:

- a 6-fold lens system composed of two different types of radiation resistant glass
- a filter assembly; the Johnson V filter has been defined with a combination of 2 different filters
- a lens barrel giving mechanical support to the lenses and ensuring their alignment.

2.3 The CCD detector

The full well capacity is the maximum number of counts measurable per single pixel, in the present case ≈120,000 cts. This parameter critically determines the dynamic range of the detector. The Analogue to Digital converters (ADCs) used in the OMC have the capability of digitizing the analogue signal coming from the CCD read-out ports to 12 bits, i.e., they provide a discrete output in up to 4096 digital levels. The ADCs are designed to be operated with 2 gain values. At the standard low gain, the full dynamic range of the CCD, 0 to 120,000 cts per pixel, is digitized into 0 to 4095 digital levels (DN), at a linear scale of ≈30 cts/DN. At high gain, which is currently used only during calibration, only the 0 to 20,000 cts per pixel range is digitized into 0 to 4095 DN, with ≈5 cts/ DN. This allows a more accurate photometry in some cases down to approximately the noise limit of the CCD. Finally, the CCD is cooled by means of a passive radiator (illustrated in Figure 1) to an operational temperature of around -80° C.

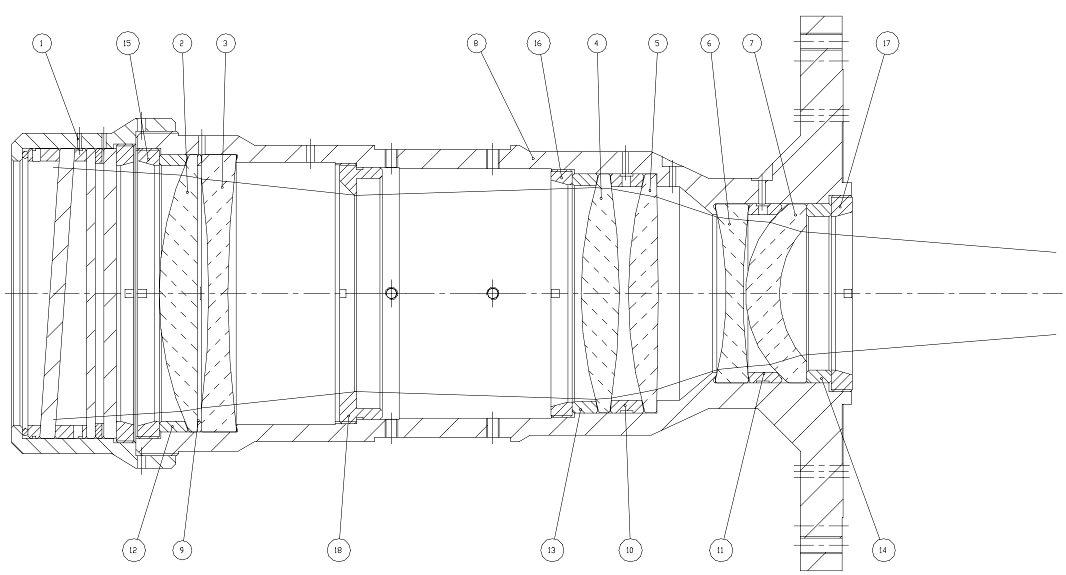

Figure 2: Optical system layout. 1: filter assembly housing; 2-7: lenses; 8: lens barrel; 9-14: spacers; 15-17: retainers; 18: aperture stop.

3 Instrument operations

Because of telemetry constraints (only ≈2.2 kbps are allocated to the OMC) it is not possible to transmit the entire OMC image to the ground. For this reason windows are selected around the proposed gamma-ray target as well as other targets of interest in the same field of view. The observers obtain the data pertinent to their target, as well as all the other OMC CCD sub-windows taken during the observation (see also the **Science Data Rights** document). These additional targets are automatically selected from the OMC "Input Catalogue". Two observation modes are available to the observer: the normal and the fast monitoring modes.

3.1 Normal science operations mode

In the normal science operations mode, the OMC monitors the optical flux of a number of targets, including the high-energy sources within its FOV, other sources of interest, stars for photometrical calibration and masked pixels from the CCD to monitor the dark current. Variable integration times during a pointing allow the monitoring of both bright and faint sources. Operations are performed automatically in the following way:

1. The sequence starts by obtaining a series of images of ≈10 ''astrometric'' reference stars, spread over the field of view. This makes it possible to measure the pointing of the OMC optical axis with an accuracy of around 0.1 pixel (≈ 2′′).
2. Then a set of photometric stars is observed (≈10 stars in the field of view with good photometric quality).
3. The CCD, centered in a target field, is then exposed with the following sequence of integration times: 10s - 50s - 200s. After each exposure the full frame is transferred to the occulted part of the chip and the next integration starts. An optimum use of the CCD, from the point of view of the noise (read-out and cosmic rays) is obtained for integration times of around 200 s, so that for the faintest objects several exposures of 200 s are summed during the analysis on ground. The number of integrations that can be added depends on the time during which the spacecraft keeps the same pointing without dithering (typically 30 min.). The brightest stars will saturate their corresponding pixels for such integration times, but the combination of short and long exposures allows to increase the magnitude range for a given field.
4. A number of windows (of typically 11×11 pixels, or ≈ 3′× 3′) are extracted around each object of interest and transmitted to the ground. When using the Proposal Generation Tool (PGT, see the **Mission Overview, Procedures and Policies** document) observers may specify a "Monitoring Window Size" for their target. The maximum allowed value is 30′, corresponding to a ≈ 30′× 30′ square window. Any value smaller than 3′ will, in fact, be executed with a 3′× 3′ window. Values greater than 3′× 3′ are executed as a mosaic of smaller windows, e.g. several 3′× 3′ windows, piled side by side, which will have to be recombined on ground. Large window sizes can be useful for targets without precise, optically measured

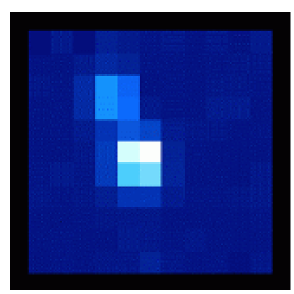

Figure 3:OMC sub-window of 11×11 pixels.

coordinates. From OSA 6.0 onwards these mosaics of sub-windows can be correctly analyzed by using IMA_wcsFlag=yes (default in OSA 7.0), once the coordinates are well defined (e.g., from X-ray observations). In this case, o_src_get_fluxes creates a virtual 11x11 pixel sub-window inside the whole area centred at the source position given in the OMC Input Catalogue. After that, OSA works on this new sub-window and ignores the previous windows of the mosaic. This is an internal software trick, these virtual sub-windows do not exist as standard sub-windows (o_ima_build, for example, will not create these virtual sub-windows as 11x11 pixel images). Note that with IMA_wcsFlag=no, these mosaics of sub-windows will not be analyzed correctly as the software treats each box individually. In addition to this method, the observer may extract the optical photometry manually from the corrected images produced by the analysis pipeline. As examples, Figure 3 shows the single OMC sub-window generated for a point source with precise coordinates like Cyg X-1, while Figure 4 displays a mosaic of 5x5 OMC sub-windows generated for the High Mass X-ray Binary 4U 1901+03 which has no accurate coordinates.

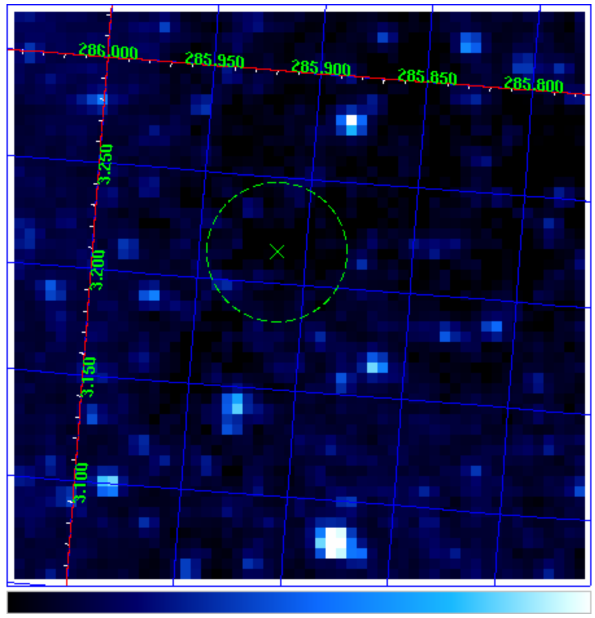

Figure 4: This image corresponds to the High Mass X-ray Binary 4U 1901+03, which generated a mosaic of 5x5 OMC sub-windows (16'x16'). The green cross and circle are the position and error of 4U 1901+03 in the IBIS catalogue, respectively.

5. Continuous monitoring of the central target with OMC will only be possible if the dithering pattern selected in the Proposal Generation Tool is none (staring) or hexagonal. In the case of larger dithering patterns, like the 5x5 one, the target will fall within the OMC field of view only for a fraction of the pointings.

3.2 Fast monitoring mode

In the normal mode it is not possible to perform a continuous monitoring with a time resolution finer than 10 seconds. Therefore, when fast variability is expected, the fast monitoring mode should be chosen. With this mode, integrations of 3 seconds are performed at intervals of 4.5 seconds and only the sections of the CCD containing the target of interest are read from the CCD and transmitted. This of course implies that the position of the source is known with an accuracy better than the window size used for fast monitoring (11×11 pixels, i.e. 3′× 3′), and that the source is bright enough to be monitored with integration times below 10 s (see Fig. 6 below).

On the other hand, note that this mode should be selected for any target brighter than V = 7.5 and fainter than V = 5.0 to avoid saturation of the CCD, whatever kind of variability is expected. Targets brighter than V= 5.0 are too bright for the OMC, even with integrations of 3 seconds.

3.3 The OMC input catalogue

As explained above, besides the proposed target(s), the OMC observes astrometric and photometric stars and other targets of scientific interest within its field of view at a given time. For this purpose, a catalogue has been compiled by the OMC team containing over 540,000 sources. It can be down-loaded by FTP (**ftp://ftp.laeff.inta.es/pub/integral/catalogue/**) and a search form is also available (**http://sdc.laeff.inta.es/omc/**).

The input catalogue includes:

- Known optical counterparts of gamma-ray sources
- Known optical counterparts of X-ray sources
- X-ray sources detected and catalogued by ROSAT
- Quasars observable with the OMC
- Additional known AGNs
- Known eruptive variable stars (including novae and cataclysmics)
- Variable objects which may require additional optical monitoring
- HIPPARCOS reference stars for positioning and photometrical calibration.

During the mission, additional sources of interest are added to the catalogue, namely:

- Newly discovered optical counterparts of high-energy sources, especially sources discovered during the Galactic Plane Survey.
- Regions of special interest for INTEGRAL science
- New supernovae
- New eruptive variable stars
- Any other Target of Opportunity (TOO).

For each scheduled observation the coordinates of all the targets of interest within the corresponding field of view are extracted from the OMC input catalogue. The table of targets of interest is included in the telecommands to be sent to the OMC before any new pointing, allowing the observer to identify all downloaded CCD windows.

3.4 Gamma-ray bursts and transient sources

The Integral Burst Alert System (IBAS) is located at the Integral Science Data Centre (ISDC) near Geneva. IBAS searches for gamma-ray bursts (GRB) using SPI/ACS triggers and IBIS/ISGRI detections and position measurements. If IBAS detects a GRB within the OMC FOV, a near-real-time command is sent to the OMC, via the Integral Mission Operations Centre (MOC), located in Darmstadt. Upon reception of this telecommand, the OMC stops the observations planned for this pointing and starts to monitor a single window of 91×91 pix (≈ 24′× 24′) around the region where the burst has been detected, with a fixed integration time of 100 s. This ‘‘trigger’’ mode is active during the rest of the pointing. The expected delay between the start of the burst and the start of OMC monitoring is less than 1 minute. Specifically, the OMC monitoring starts less than 15 seconds after the IBAS trigger. This makes it possible to obtain slightly delayed but simultaneous optical, X-ray and gamma-ray data of any burst taking place within the OMC FOV.

The **Science Data Rights** document describes how and under which conditions the OMC data are distributed to the observers in the case of a gamma-ray burst or a transient.

4 Instrument performances

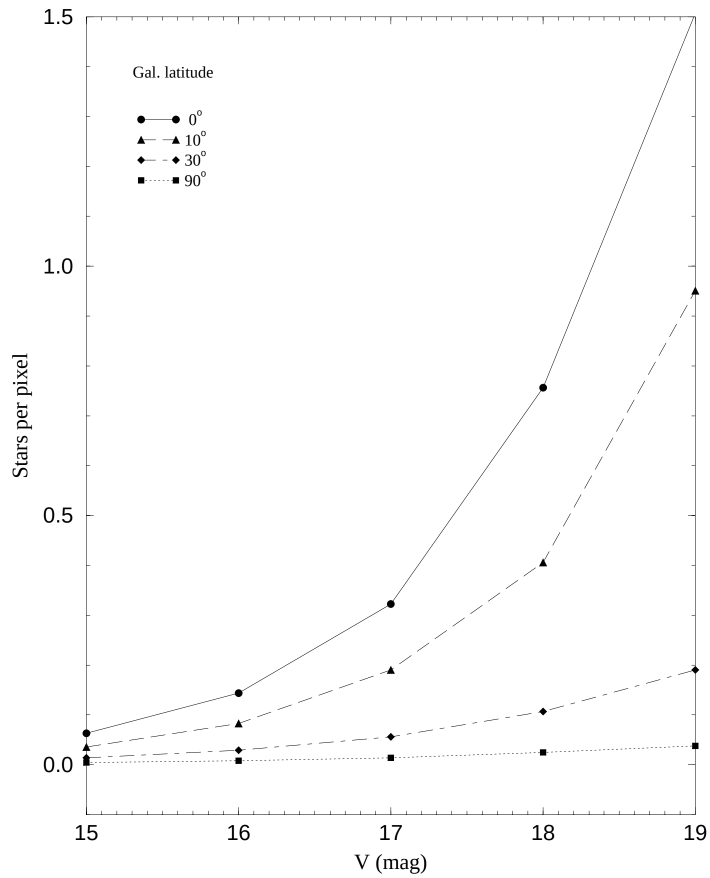

Figure 5: Average number of stars per pixel brighter than a given V magnitude at different galactic latitudes.

4.1 Background and read-out noise

There are two main sources of background flux for the OMC, both related to the rather large angular pixel size of 17.5′′× 17.5′′: scattered sunlight (zodiacal light) and unresolved stellar sources. Maximum background conditions correspond to pointings towards the galactic plane with maximum zodiacal light, while the minimum background is achieved around the galactic pole with minimum zodiacal light. Figure 5 shows the average number of stars brighter than a given magnitude contained within a single OMC pixel. It can be seen that, on average, no source confusion occurs for objects brighter than m_V =17 at any galactic latitude. For m_V = 18.0 source confusion can become problematic in some regions very close to the galactic plane. It is important to stress that on the galactic plane there are on average more than one star per pixel with m_V between 17 and 19. The density of stars on the galactic plane indeed determines the limiting magnitude of the instrument. At galactic latitudes |b|>30° the problem of source confusion becomes negligible, except for specific cases in which bright stars are separated by just a few arcseconds. The background measured in orbit corresponds well to the expected values.

The read-out noise of the OMC as measured on ground is between 1-1.5 DNs/pixel (digital levels) for low gain and between 3-3.5 DNs/pixel in high gain, corresponding to 30-45 cts and 15-17 cts respectively. The read-out noise measured in orbit is consistent with these values.

4.2 Limiting faint magnitude

Assuming a minimum level of background (see the definition in the previous section) and a combination of 10 exposures of 200 s each, the limiting magnitude of the OMC is found to be **m_V = 18.1** (3 σ detection level). This value corresponds to a limiting sensitivity of the instrument of 2.1×10^{-16} erg cm^{-2} s^{-1} Å^{-1} or, alternately, 5.8×10^{-5} ph cm^{-2} s^{-1} Å^{-1} , at 550 nm. At a maximum background level (as defined above) the limiting magnitude is **m_V = 17.5**. Note that these sensitivities can only be achieved for isolated stars for which the background can be properly estimated. Figure 6 shows the limiting faint magnitude for both maximum and minimum background as a function of integration time, assuming in all cases that 10 images have been combined to increase the signal to noise ratio. Figure 7 shows the limiting magnitude in best background conditions, and for different combinations of exposures.

Measurements in orbit show that the OMC is in average about 30% more sensitive than estimated during ground-based calibrations. However, the absolute photometric calibration changes with time and is continuously updated by the OMC team.

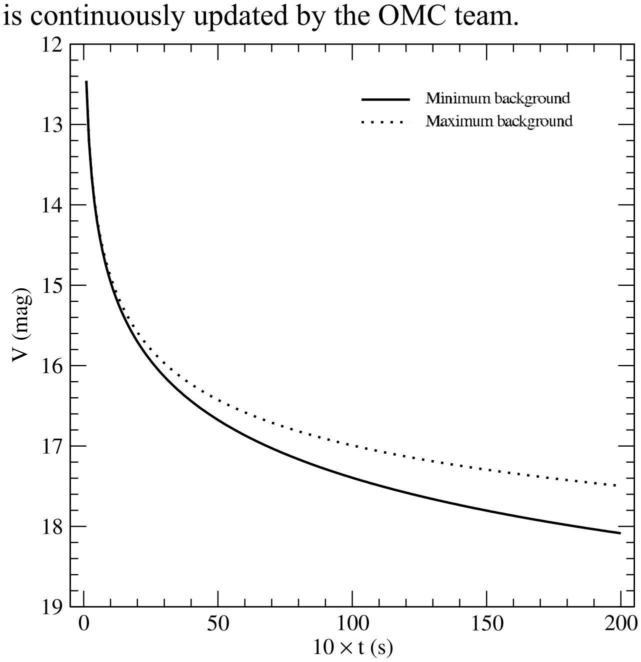

Figure 6: Limiting faint magnitude for a 3σ detection in the V band as a function of integration time. The best and the worst background cases are shown. It is assumed that 10 separate exposures, each with the integration time as given in the plot, have been combined together in order to increase the signal to noise ratio.

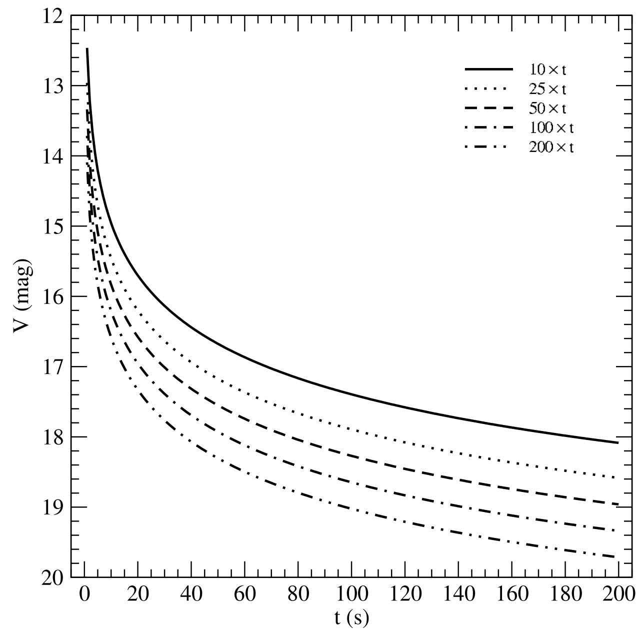

Figure 7: Limiting faint magnitude for a 3σ detection in the V band as a function of integration time. Best case background conditions are assumed (galactic pole, no zodiacal light). The curves correspond to different total numbers of images being combined.

4.3 Limiting bright magnitude

The full well capacity of the CCD constrains the magnitude of the brightest stars that can be measured without pixel saturation for a given integration time. With 10 s integrations, the central pixel becomes saturated for objects brighter than m_V=7. With integrations of 200 s, even stars with $m_V \approx 10$ will start to saturate the CCD. Severe saturation of the CCD might imply losing the information from the surrounding pixels and potentially from the column containing the source, but no damage is expected on the detector. Figure 8 shows the predicted number of counts on the CCD as a function of V magnitude for a 10s integration. This number corresponds to the counts expected in the central (brightest) pixel only. Finally, Figure 9 gives the integration time at which stars of different magnitudes will start to saturate the CCD.

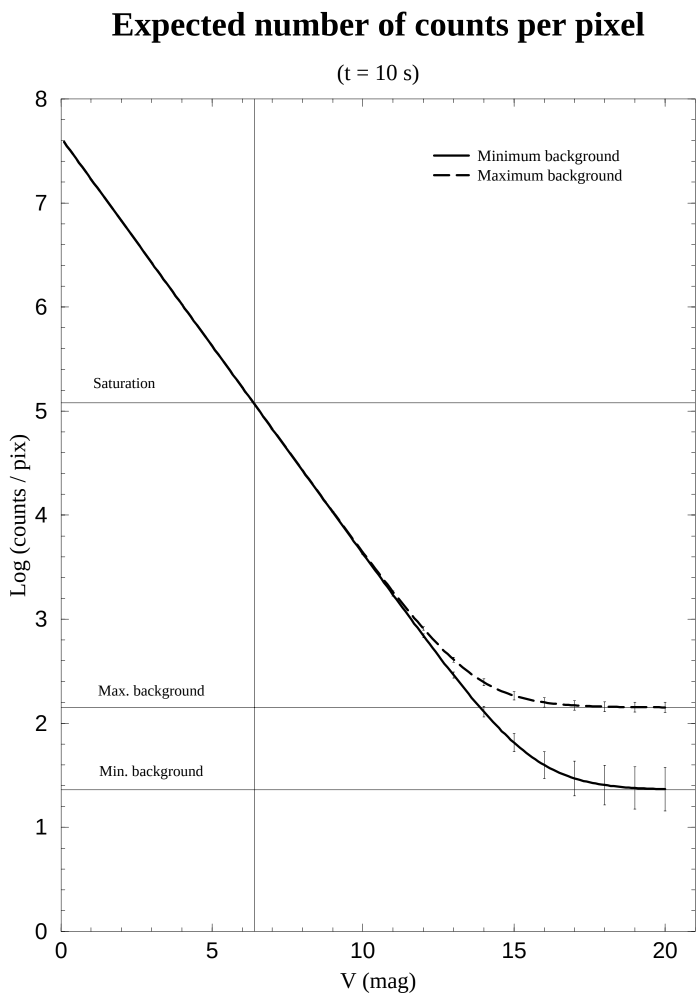

Figure 8: Expected number of counts on the central brightest pixel as a function of V magnitude, for an integration time of 10 s. The error bars correspond to 1σ. The plot also includes the expected background flux computed for maximum and minimum conditions.

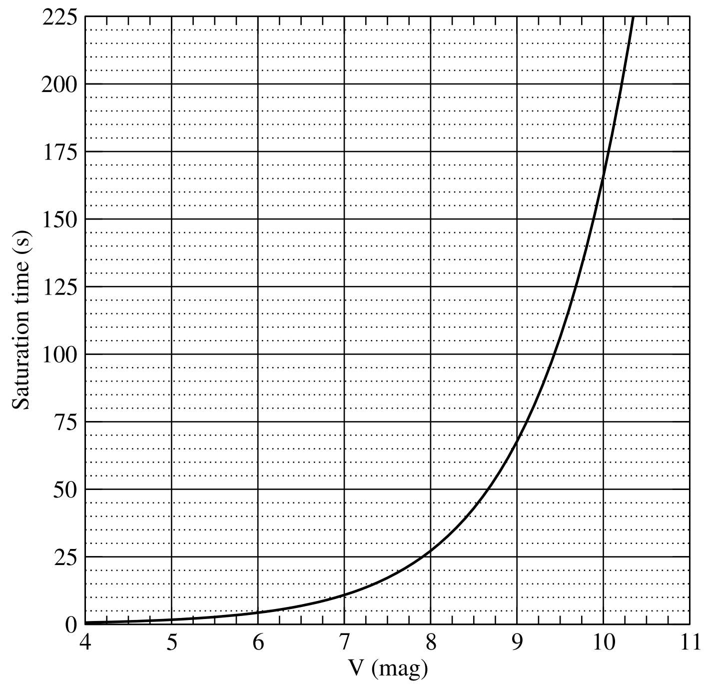

Figure 9: CCD saturation time as a function of V magnitude. Note that for integrations of 50 s, all stars with m_V<8.6 will saturate the CCD. For the shortest OMC integration times (fast moniroting mode: 3 seconds), the brightest stars that can be observed should be fainter than m_V>5.

4.4 Photometric accuracy

Table 2 shows the expected error (expressed in magnitudes) of a given measurement for various “effective” integration times and magnitudes. "Effective" integration time means the total exposure after combining several shots. The value of 300 seconds corresponds to the "typical effective exposure" obtained by the OMC Standard Analysis at ISDC using the default parameters. A value around 900 seconds corresponds to the maximum effective exposure one can get in the OMC Standard Analysis (when changing the default parameters). 900 seconds of effective exposure is also a representative value for an entire 5x5 dither pattern (~2000s pointing). Of course, these values should be used as a guide: they are the best results that can be obtained with the latest version of the analysis software and are only valid for isolated stars in “Staring” mode.

The values for photometric accuracy have been computed by taking into account the most current knowledge of the OMC instrument. One can see in Table 2 that good photometry can be performed in the V band for objects of quite different brightnesses. Note that these accuracies can only be obtained for isolated stars for which the background can be properly estimated. Furthermore, in case of dithering the photometric dispersion is >0.02 (mag.) in all cases. This value (0.02) is the accuracy of the OMC flatfield matrix. So, if the source is observed in different detector pixels, as occurs for a dithered observation, the accuracy of the flatfield produces an additional scattering on the observed magnitudes of about 0.02 mag.

Table 2: Photometric accuracy for different background levels (in units of magnitude)

6. **source** $m_V \rightarrow$	**8**	**10**	**12**	**14**	**16**
effective[3] exposures	assuming a typical background level:				
10 s	0.007	0.02	0.1	-	-
300 s	-	0.005	0.01	0.045	0.3
900 s	-	0.003	0.006	0.026	0.17

4.5 Focusing

The focusing capabilities of the OMC system depend very slightly on the lens temperature and the pixel location over the detector. The PSF follows a Gaussian distribution whose FWHM remains in the range 1.2 to 1.4 pixels in most cases, as shown in Figure 10

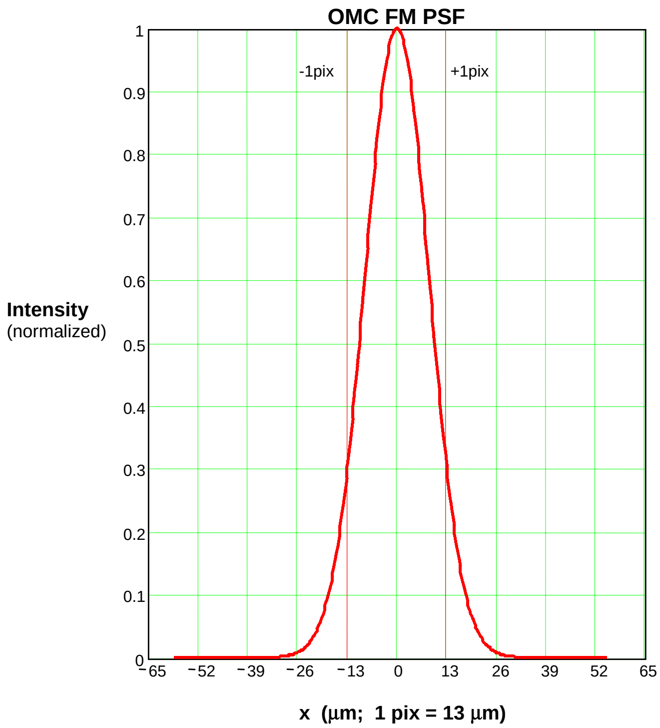

Figure 10: Point Spread Function of the OMC (optical system + detector). The plot shows a fit to the average PSF measured under different conditions. The PSF measured in orbit follows a Gaussian with FWHM > 1.3 pixels. More than 90% of the energy falls within 3×3 pixels.

[3]See text for the definition of an “effective” exposure.

5 Data products

5.1 Overview of the scientific analysis

The scientific analysis of all the INTEGRAL instruments is split into a number of steps with similar tasks:

COR - Data Correction

At this step the appropriate calibration data (dark current, bias, flat-field) for the current science window group are selected and the corrected pixel values for the subsequent analysis are calculated.

GTI - Good Time Handling

At this step Good Time Intervals (GTI) for the current Science Window are derived, based on housekeeping data and attitude information.

IMA - Source Flux Reconstruction and Image Creation

At this step the fluxes of the individual sources are calculated and the source magnitudes are derived. The user can also require to build the individual images containing the OMC boxes at this step.

Observers will receive the results from all of these steps:

The raw and corrected CCD sub-windows for all pre-defined sources in the field of view. The data are provided in a tabulated format with pixel values as vector entries in a column of the tables. CCD corrected windows will include flat-field calibration and dark current subtraction, but not the removal of cosmic rays.

In addition, a series of tables with derived fluxes and magnitudes for all observed sources as a function of time. By default, photometrical analysis will be performed combining all images obtained within periods of around 10 minutes.

IMA2 - Results Collection

The data concerning one observation are distributed between different files and Science Windows. At this step the OMC flux results are collected into a single table.

The Off-line Scientific Analysis allows the observers to reprocess the OMC data with different parameters as, for example, the sampling time or more recent calibration files. Figure 11, Figure 12 and Figure 13 show three examples of OMC light curves. It can be seen that good photometric results can be obtained for a variety of objects, even with the presence of a close companion as occurs in the case of Cyg X-1.

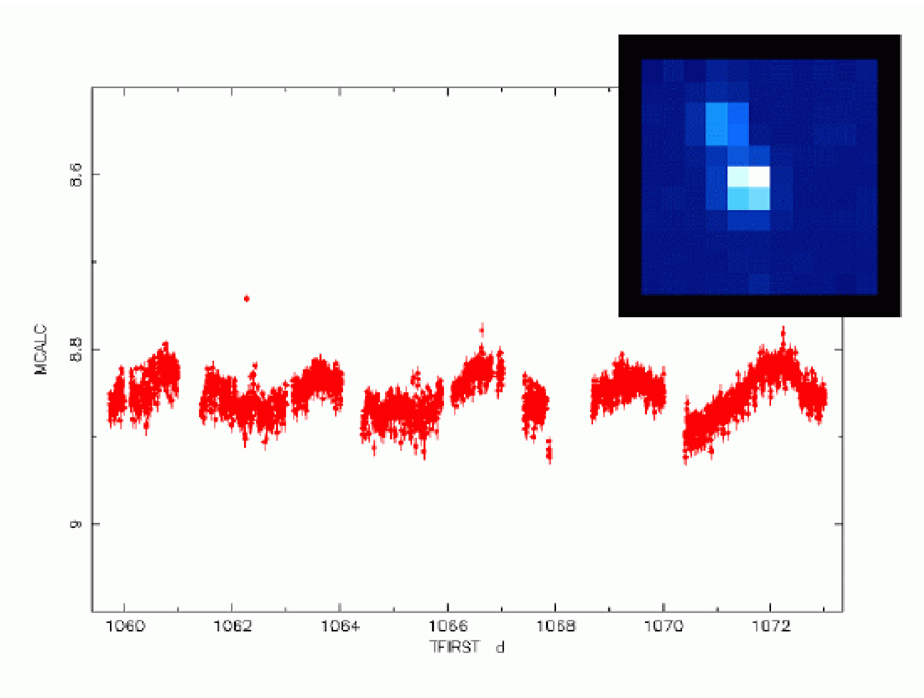

Figure 11: Computed light curve for Cyg X-1 using single exposures of 10 and 30 seconds. The OMC sub-window for Cyg X-1 is shown on the upper right corner of the graph.

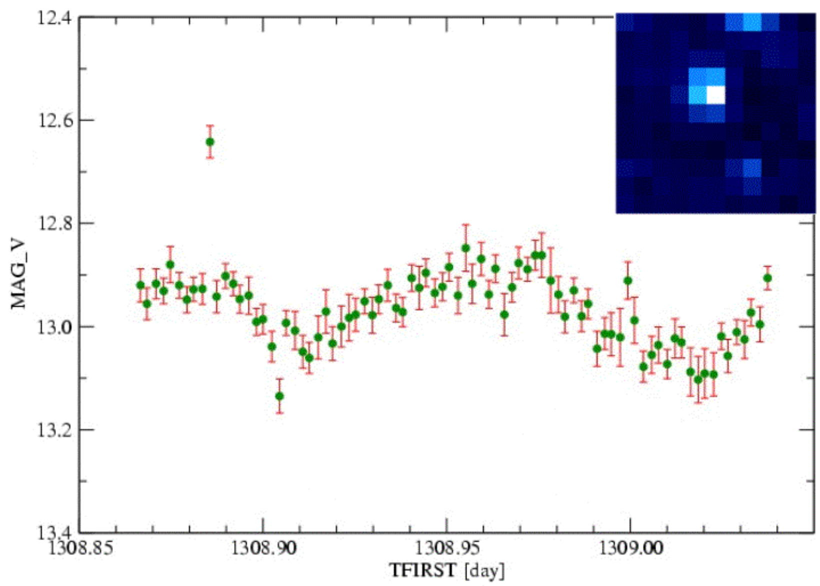

Figure 12: OMC light curve of the Low Mass X-ray Binary Sco X-1. It includes only single exposures of 100 seconds. The downloaded OMC sub-window for this source is also shown on the upper right corner of the graph.

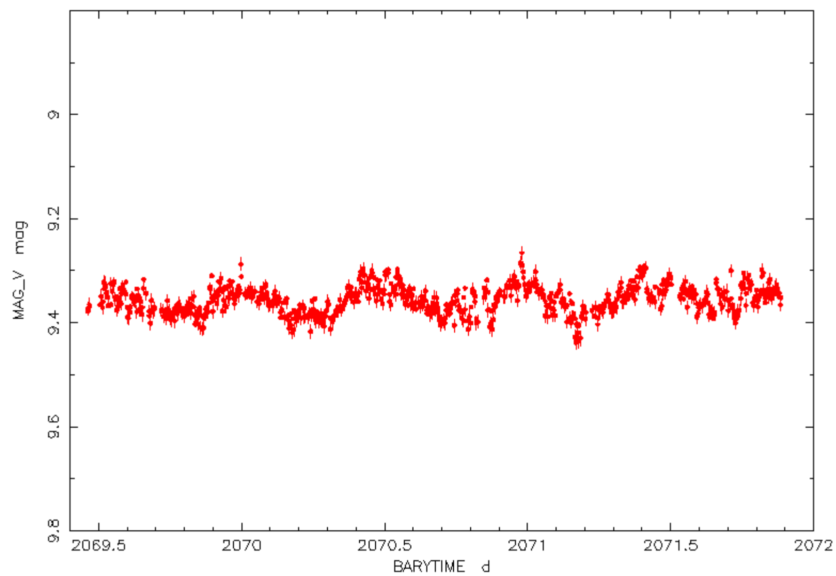

Figure 13: OMC light curve during an Integral TOO observation of the Be/X-ray binary 3A 0535+262, obtained by using single exposures of 10 and 50 seconds. It shows small variability typical of Be systems.

5.2 Known limitations

1. The automatic extraction of fluxes and magnitudes produces reliable results only for point-like sources.
2. If the source coordinates are inaccurate by more than 2 OMC pixels (≈35"), the analysis software will not be able to re-centre the target and the derived fluxes and magnitudes obtained with the default analysis parameters will not be correct.
3. For extended sources or high-energy source counterparts with large uncertainties in their position, the OMC planning assigns multiple adjacent sub-windows to cover the whole area. In that case, multiple boxes are found with different ranks but with the same OMC_ID. From OSA 6.0 onwards these adjacent sub-windows can be correctly analyzed by using IMA_wcsFlag=yes (default in OSA 7.0). In this case, o_src_get_fluxes creates a virtual 11x11 pixel sub-window inside the whole area centred at the source position. After that, OSA works on this new sub-window and ignores the previous sub-windows mosaic. This is an internal software trick, these virtual sub-windows do not exist as standard sub-windows (o_ima_build, for example, will not create these virtual sub-windows as 11x11 pixel images). Note that with IMA_wcsFlag=no, these adjacent sub-windows will not be analyzed correctly as the software treats each box individually.
4. If another star is within a few pixels of the source of interest, it can introduce systematic errors in the derived fluxes and magnitudes. The strength of this effect can be different

for different pointings, since the relative position in the sub-windows will change slightly for different rotation angles.

5. Some of the bright sources slightly saturating one or a few pixels might not be detected as saturated sources. As a consequence, their derived magnitudes are not correctly computed. The observer should check in Table 7 whether the source might be saturating the CCD for a given integration time, and re-analyze the data rejecting the shots with the longest integration times.
6. Due to thermo-elastic deformations, the alignment of the OMC optical axis with the spacecraft attitude reference (after correcting for the known OMC misalignment) may diverge by up to 30” (~2 pixels). This is corrected for in the analysis (OSA 5 upwards) using the photometric reference stars, giving an accuracy of ≤2” in most cases.